Sterile Neutrino Decays Face Constraints on the Flux of $\overline{\nu}_e$ from the Sun

Matheus Hostert[1, 2, 3, *] and Maxim Pospelov[1, 2, 3, †]

[1] *School of Physics and Astronomy, University of Minnesota, Minneapolis, MN 55455, USA*
[2] *William I. Fine Theoretical Physics Institute, School of Physics and Astronomy, University of Minnesota, Minneapolis, MN 55455, USA*
[3] *Perimeter Institute for Theoretical Physics, Waterloo, ON N2J 2W9, Canada*

(Dated: November 18, 2019)

I. INTRODUCTION

On average, solar neutrinos provide the largest flux of neutrinos on the Earth (for a nice overview of neutrino sources see Ref. [1]).

The most stringent upper limits on an undistorted flux of solar $\overline{\nu_e}$ from ^8B are given by KamLAND [2]

$$P^{\rm KamLAND}_{\nu_e\to\overline{\nu_e}}(E_\nu \geq 8.3\ {\rm MeV}) < 5.3\times 10^{-5}, \tag{1}$$

and Borexino [3]

$$P^{\rm Borexino}_{\nu_e\to\overline{\nu_e}}(E_\nu \geq 1.8\ {\rm MeV}) < 7.2\times 10^{-5}. \tag{2}$$

SuperKamiokande (SK) also provides limits at the highest energies, with the most stringent bounds coming from a preliminary analysis of all SK-IV data [4]

$$P^{\rm SK-IV}_{\nu_e\to\overline{\nu_e}}(E_\nu \geq 9.3\ {\rm MeV}) \lesssim 1.0\times 10^{-4}. \tag{3}$$

In addition to these, SNO has also set limits at the level of $P^{\rm SNO}_{\nu_e\to\overline{\nu_e}}(E_\nu \in [4, 14.8]\ {\rm MeV}) < 8.3\times 10^{-3}$ [5]. All the limits are at 90 C.L. and assume a total ^8B flux of $5.94\times 10^6\ {\rm cm}^{-2}\ {\rm s}^{-1}$. At the lowest energies, a bound can also be obtained by noting that the number of $\nu - e$ scattering events in solar neutrino experiments decreases if too many ν_4 are produced, both due to lower cross sections and suppressed production. These effects, however, are insensitive to variations of the total ν_e flux below the percent level.

The decay of active neutrinos to invisible final states has received great interest in the past [6, 7]. [8] $\nu_4\to\overline{\nu_e}\phi$ in the context of a 17 keV sterile and Majoron models. Here, for the first time, we consider antineutrinos produced in an intermediate decay, namely, $\nu_4\to\nu_\alpha\phi\to\nu_e\nu_e\overline{\nu_e}$.

II. VISIBLE NEUTRINO DECAYS

Our analysis is restricted to the Dirac neutrino case, although our bounds would be even stronger if neutrinos were Majorana. This is because the lepton number violating decays $\nu_4\to\overline{\nu_e}B$ would be allowed, providing an even larger source of solar $\overline{\nu_e}$.

Due to mixing, sterile neutrinos with masses below the MeV would be produced in the Sun via the same processes responsible for ν_e production at a rate $|U_{e4}|^2$ times smaller. Once produced, the ν_4 mass eigenstates immediately decay to a massless neutrino and a boson, which may be a scalar or a vector boson. The boson then promptly decays to a neutrino-antineutrino pair, giving rise to our signal. Overall, the process of interest is

$$\begin{aligned}\nu_4(E_\nu)\ \to\ \nu_e(E_1)\ +\ B(E_B)\\ \searrow \nu_e(E_2)\ +\ \overline{\nu_e}(E_3).\end{aligned} \tag{4}$$

We now summarize the decay rates for a heavy Dirac neutrino decaying to a mass active neutrino flavour, and a boson B, quoting the results for the scalar $B=\phi$ and vector $B=Z'$ cases. The heavy neutrino is assumed to be polarised with a definite helicity h. For most cases of interest, $E_\nu \gg m_4$, so if ν_4 is produced in Weak interactions, the right-handed ν_4 population is negligible. Nevertheless, due to the assumption of parity conservation for the B interactions with neutrinos, one can compute the helicity flipping (HF) and helicity conserving (HC) decay channels by noting that

$$\begin{aligned} d\Gamma(\nu_4^{h=-1}\to\nu_L B) &= d\Gamma(\nu_4^{h=1}\to\nu_R B),\\ d\Gamma(\nu_4^{h=1}\to\nu_L B) &= d\Gamma(\nu_4^{h=-1}\to\nu_R B).\end{aligned} \tag{5}$$

In this way, all HF decay rates are given by $d\Gamma(\nu_4^{h=1}\to\nu_L B)$ and all HC channels by $d\Gamma(\nu_4^{h=-1}\to\nu_L B)$. Assuming heavy neutrinos to be ultra-relativistic, we find the decay rates below, in agreement with Refs [].

$\underline{\nu_4^h\to\nu_L\phi}$:

$$|\mathcal{M}_h|^2 = \frac{m_4^2}{2}\left[(1+h)(1-r^2) + 2h\frac{E_1}{E_\nu}\right] \tag{6}$$

$\underline{\nu_4^h\to\nu_L Z'}$:

$$\begin{aligned}|\mathcal{M}_h|^2 = \frac{m_4^2(1-r^2)}{2r^2}\Bigg[&(1-h) + (1+h)2r^2\\ &- 2h\frac{E_1}{E_\nu}\frac{1-2r^2}{1-r^2}\Bigg].\end{aligned} \tag{7}$$

* mhostert@umn.edu
†

III. THE SIGNAL

To leading order in the small mixing angles, the number of IBD events in a given experiment can be computed as

$$\frac{\mathrm{d}N_{\mathrm{events}}}{\mathrm{d}E_\nu\,\mathrm{d}E_1\,\mathrm{d}E_3} = \mathcal{N}\,\frac{\mathrm{d}\Phi^{\nu_4}}{\mathrm{d}E_\nu}\,\frac{\mathrm{d}P^{\mathrm{dec}}}{\mathrm{d}E_1\mathrm{d}E_3}\,\sigma^{\mathrm{IBD}}(E_3)\,\overline{P_{ee}}(E_3), \tag{8}$$

where $\mathcal{N}$ stands for total exposure of the experiment and

$$\frac{\mathrm{d}\Phi^{\nu_4}}{\mathrm{d}E_\nu} = |U_{e4}|^2\frac{\mathrm{d}\Phi^{\nu_e}}{\mathrm{d}E_\nu}, \tag{9}$$
$$\frac{\mathrm{d}P^{\mathrm{dec}}}{\mathrm{d}E_1\mathrm{d}E_3} = \frac{1}{\Gamma_{\nu_h}\Gamma_{Z'}}\frac{\mathrm{d}\Gamma_{\nu_h\to\nu_e Z'}}{\mathrm{d}E_1}\frac{\mathrm{d}\Gamma_{Z'\to\nu_e\overline{\nu_e}}}{\mathrm{d}E_2}.$$

Note that Eq. (8) is the analogue of Eq. (18) from Ref. [9], and is simpler since we work with very long baselines and under the assumption that the number of initial ν_μ states is negligible.

Inverse beta decay (IBD) of free protons has a large cross section for MeV electron antineutrinos and is the primary detection channel for reactor neutrinos. If compared to to the neutrino-electron elastic scattering cross section (see Fig. 1), it is orders of magnitude larger and offers a much cleaner signal. After produced, the positron annihilates and the final state neutron is quickly captured by Hydrogen. This results in a double-bang signature with the positron kinetic energy $T_e = E_\nu - 1.8$ MeV, and a later emission of a ≈ 2.2 MeV gamma which greatly reduces backgrounds. The cross section for this process is well understood at high [10] and low [11] energies, and relatively simple formulae that are valid at all energies have been provided by Ref. [12]. Here we implement the latter calculation, which is provided as machine-friendly data files by Ref. [13].

The largest flux of solar neutrinos at the energies we are interested comes from ^8B. This has been extensively studied in the literature, and here we implement the fluxes provided in Ref. [14]. For the total flux from ^8B and its uncertainty, we use the high-metallicity fluxes from Ref. [15].

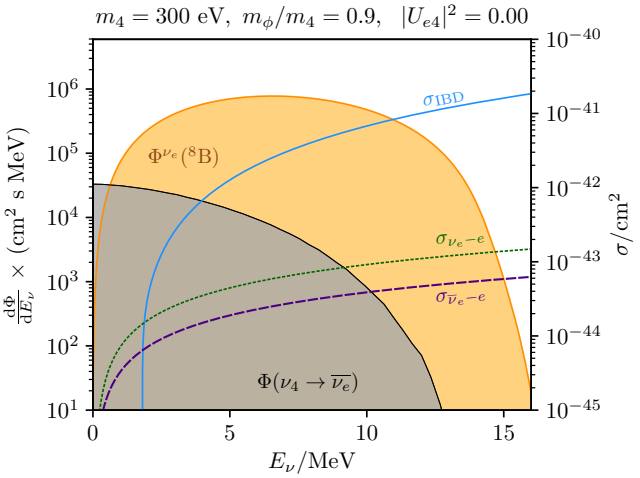

FIG. 1. The solar neutrino energy spectrum from ^8B (shaded orange) and from the decays of ν_h (shaded grey). We also show the inverse beta decay (IBD) and neutrino-electron scattering cross sections on an overlaid axis.

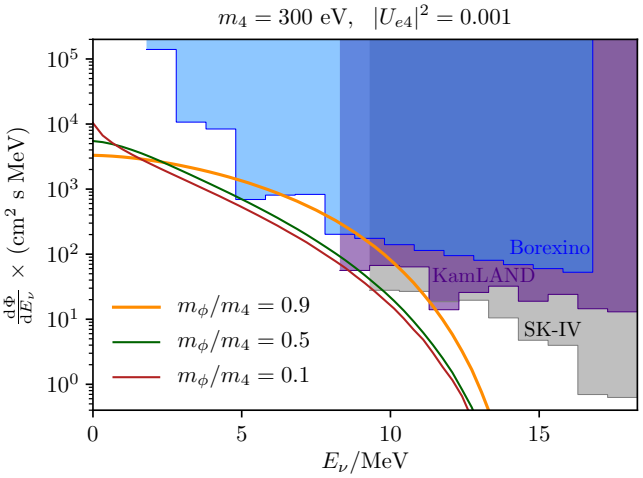

FIG. 2. The experimental limits on solar $\overline{\nu_e}$ at 90% C.L. as a function of the neutrino energy. The shaded regions are excluded by Borexino (blue), KamLAND (purple) and SuperK-IV (grey). Three different new physics predictions are also shown as solid curves assuming $|U_{\mu_4}| = |U_{\tau 4}| = 0$.

IV. RESULTS

V. FURTHER CONSEQUENCES

a. SN1987A neutrino events lack of events + time delay

b. Cosmology

VI. CONCLUSIONS

As pointed out by Li *et al*, JUNO will be able to improve on such limits [16].

SuperKamiokande with Gd – lower thresholds and larger efficiency. In fact, the presence of Gd would allow SuperK to lower the $\overline{\nu_e}$ detection threshold to neutrino energies as low as the IBD threshold provided $E_e > 0.8$ MeV [17].

THEIA?

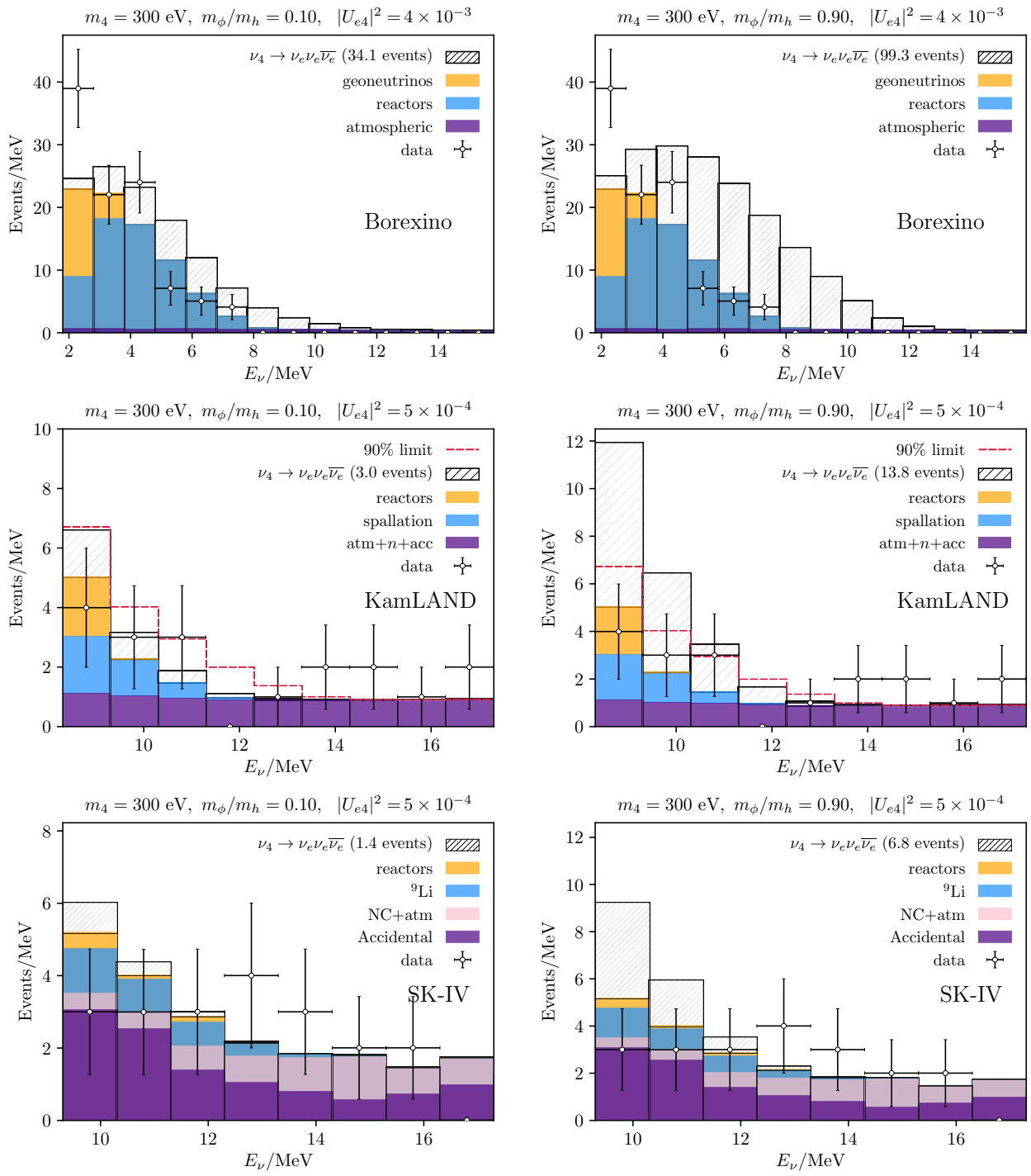

FIG. 3. The inverse beta decay spectrum at KamLAND (top row) and Borexino (bottom row) as stacked histograms. The filled histograms show the background estimations by the collaboration, and the hashed histogram the prediction of visible neutrino decays. For KamLAND, we also show the 90% C.L. upper limit on the event spectra provided by the collaboration. All plots assume $|U_{\mu 4}| = |U_{\tau 4}| = 0$.

ACKNOWLEDGMENTS

Appendix A: Visible Decays

We now summarise the decay rates for a heavy Dirac neutrino decaying to a mass active neutrino flavour, and a boson B, quoting the results for the scalar ($B = \phi$) and vector ($B = Z'$) cases. The heavy neutrino is assumed to be polarised with a definite helicity h. For most cases of interest, $E_\nu \gg m_4$, so if ν_4 is produced in Weak interactions, the right-handed ν_4 population

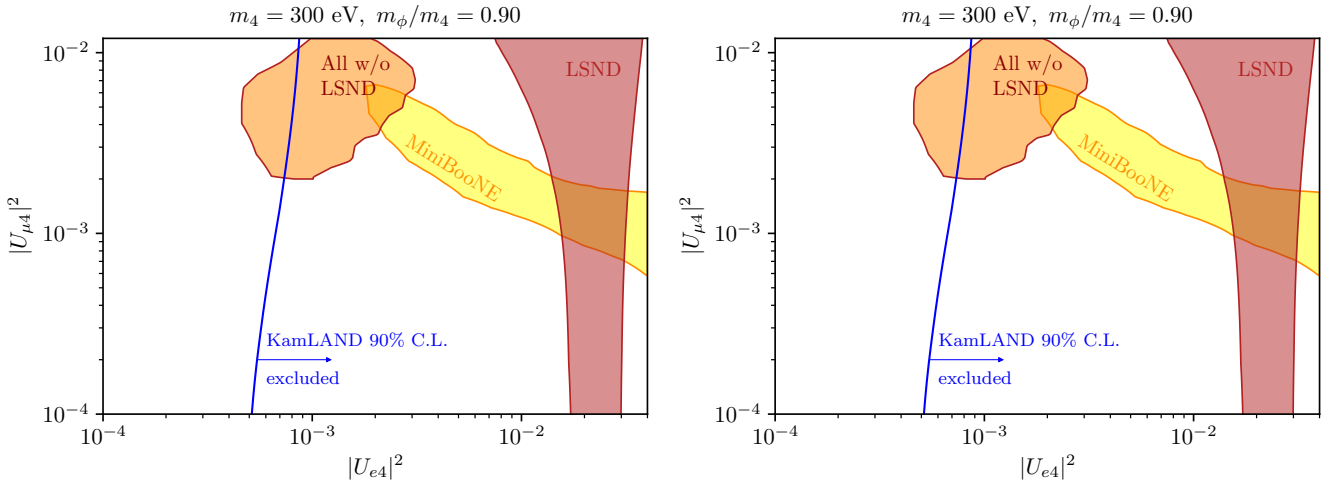

FIG. 4.

is negligible. Nevertheless, due to the assumption of parity conservation for the B interactions with neutrinos, one can compute the helicity flipping (HF) and helicity conserving (HC) decay channels by noting that $d\Gamma(\nu_4^{h=-1} \to \nu_L B) = d\Gamma(\nu_4^{h=1} \to \nu_R B)$ and $d\Gamma(\nu_4^{h=1} \to \nu_L B) = d\Gamma(\nu_4^{h=-1} \to \nu_R B)$. In this way, all HF decay rates are given by $d\Gamma(\nu_4^{h=1} \to \nu_L B)$ and all HC channels by $d\Gamma(\nu_4^{h=-1} \to \nu_L B)$. Our results are shown below.

$\underline{\nu_4^h \to \nu\phi}$:

$$\begin{aligned} |\mathcal{M}_h|^2 &= \frac{m_4^2}{2}(1-r^2)(1-h\cos\theta) \\ &= \frac{m_4^2}{2}\left((1+h)(1-r^2) + 2h\frac{E_1}{E_\nu}\right) \\ &= m_4^2 \begin{cases} \frac{E_1}{E_\nu} & \text{for } h=-1 \\ 1-\frac{E_1}{E_\nu} - r^2 & \text{for } h=1 \end{cases} \end{aligned} \tag{A1}$$

$\underline{\nu_4^h \to \nu Z'}$:

$$\begin{aligned} |\mathcal{M}_h|^2 &= m_4^2(1-r^2)\left(1 - h\cos\theta + \frac{1+h\cos\theta}{2r^2}\right) \\ &= \frac{m_4^2(1-r^2)}{2r^2}\left((1-h) + (1+h)2r^2 - 2h\frac{E_1}{E_\nu}\frac{1-2r^2}{1-r^2}\right) \\ &= \frac{m_h^2}{r^2} \begin{cases} 1-\frac{E_1}{E_\nu} - r^2\left(1-2\frac{E_1}{E_\nu}\right) & \text{for } h=-1 \\ \frac{E_1}{E_\nu} + 2r^2\left(1-\frac{E_1}{E_\nu} - r^2\right) & \text{for } h=1 \end{cases} \end{aligned} \tag{A2}$$

We assume the heavy neutrinos are ultra-relativistic, so that we are justified in using

$$E_1 = \frac{E_\nu}{2}(1-r^2)(1+\cos\theta). \tag{A3}$$

Appendix B: Solar Flavour Transitions

Once produced from the ν_4 decay, the active neutrinos propagate from the Sun's core to the Earth, subject to matter effects. The flavour evolution of these neutrinos is given by the well-known LMA-MSW solution []. Here, we are primarily interested in the total $\overline{\nu_e}$ flux that exits the Sun, so all antineutrinos produced in the decay of the boson B contribute. In what follows, we will assume that $|U_{\mu 4}| = |U_{\tau 4}|$ for simplicity.

To a very good approximation, the flavour transitions of neutrinos in the Sun can be taken to be adiabatic []. In this limit, the relevant flavour conversion probabilities are for a ν_α to convert into a ν_β, $P_{\alpha\beta}$, are given by

$$\begin{aligned} P_{ee}(E_\nu) &\approx c_{13}^4\left(\frac{1}{2} + \frac{1}{2}\cos 2\theta_{12}\cos 2\theta_{12}^M\right) + s_{13}^4, \\ P_{\mu e}(E_\nu) + P_{\tau e}(E_\nu) &= 1 - P_{ee}(E_\nu), \end{aligned} \tag{B1}$$

with their antineutrino $\overline{P}_{\alpha\beta}$ analogue. Here, θ_{12}^M is the solar mixing angle in matter at the core, defined as

$$\tan 2\theta_{12}^M = \frac{\sin 2\theta_{12}\Delta m_{12}^2}{\Delta m_{12}^2\cos 2\theta_{12} - A_{\rm CC}}, \tag{B2}$$

with $A = \pm 2\sqrt{2}E_\nu G_F N_e(0)$ for neutrinos (antineutrinos). It is easy to see that while ν_e states undergo the usual MSW transition, having enhanced flavour transitions due to adiabatic conversions above the resonance, $P_{ee}(5\text{ MeV}) \approx 0.32$, the $\overline{\nu_e}$ states do not. Instead, $\overline{\nu_e}$ change flavour less often above the resonance and have enhanced survival probabilities, $\overline{P}_{ee}(5\text{ MeV}) \approx 0.64$. The full flavour transition probability is shown in Fig. 5.

Finally, we may also compute $\overline{P_{\mu e}}$ by noting that within the two flavour approximation the T symmetry always holds ($P_{\alpha\beta} = P_{\beta\alpha}$). This is a consequence of the unitarity of the Hamiltonian, and holds even for non-symmetric matter profiles, such as the Sun [18, 19]. Hence, the CPT asymmetry is equivalent to the CP asymmetry $P_{\alpha\beta} - \overline{P_{\alpha\beta}}$, such that $\overline{P_{\mu e}} = \overline{P_{e\mu}}$.

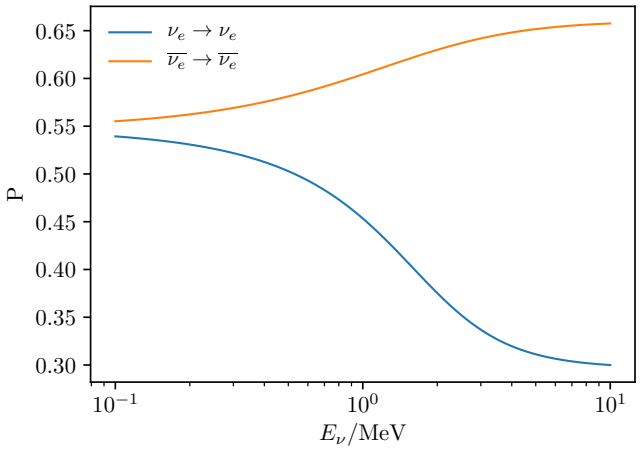

FIG. 5. Caption

Appendix C: Statistical Method

When deriving upper limits on the mixing angles, we minimize the following log-likelihood function

$$\mathcal{L} = 2\sum_i \left[\mu_i(\vec{\theta},\vec{\beta}) - D_i + D_i \ln \frac{D_i}{\mu_i(\vec{\theta},\vec{\beta})}\right] + \sum_j \frac{\beta_j^2}{\sigma_j^2}, \tag{C1}$$

where $\vec{\theta}$ stands for the vector of physics parameters (*e.g.*, $|U_\alpha|^2$), $\vec{\beta}$ the vector of nuisance parameters with individual entries β_j and associated Gaussian errors σ_j. As an approximation, we assume $\mathcal{L}$ to follow a χ^2 distribution when estimating our confidence intervals.

The most important systematics for our study are the uncertainties on the total ^8B solar neutrino flux and total backgrounds numbers. We assume an overall

[1] E. Vitagliano, I. Tamborra, and G. Raffelt, (2019), arXiv:1910.11878 [astro-ph.HE].
[2] A. Gando *et al.* (KamLAND), Astrophys. J. **745**, 193 (2012), arXiv:1105.3516 [astro-ph.HE].
[3] M. Agostini *et al.* (Borexino), (2019), arXiv:1909.02422 [hep-ex].
[4] W. Linyan, *Experimental Studies on Low Energy Electron Antineutrinos and Related Physics*, Ph.D. thesis, Tsinghua University (2018), available at http://www-sk.icrr.u-tokyo.ac.jp/sk/_pdf/articles/2019/SKver-Linyan.pdf.
[5] B. Aharmim *et al.* (SNO), Phys. Rev. **D70**, 093014 (2004), arXiv:hep-ex/0407029 [hep-ex].
[6] A. S. Joshipura, E. Masso, and S. Mohanty, Phys. Rev. **D66**, 113008 (2002), arXiv:hep-ph/0203181 [hep-ph].
[7] J. F. Beacom and N. F. Bell, Phys. Rev. **D65**, 113009 (2002), arXiv:hep-ph/0204111 [hep-ph].
[8] Z. G. Berezhiani, G. Fiorentini, M. Moretti, and A. Rossi, Z. Phys. **C54**, 581 (1992).
[9] M. Dentler, I. Esteban, J. Kopp, and P. Machado, (2019), arXiv:1911.01427 [hep-ph].
[10] C. H. Llewellyn Smith, *Gauge Theories and Neutrino Physics, Jacob, 1978:0175*, Phys. Rept. **3**, 261 (1972).
[11] P. Vogel and J. F. Beacom, Phys. Rev. **D60**, 053003 (1999), arXiv:hep-ph/9903554 [hep-ph].
[12] A. Strumia and F. Vissani, Phys. Lett. **B564**, 42 (2003), arXiv:astro-ph/0302055 [astro-ph].
[13] A. M. Ankowski, (2016), arXiv:1601.06169 [hep-ph].
[14] J. N. Bahcall, E. Lisi, D. E. Alburger, L. De Braeckeleer, S. J. Freedman, and J. Napolitano, Phys. Rev. **C54**, 411 (1996), arXiv:nucl-th/9601044 [nucl-th].
[15] C. Pena-Garay and A. Serenelli, (2008), arXiv:0811.2424 [astro-ph].
[16] S. J. Li, J. J. Ling, N. Raper, and M. V. Smirnov, Nucl. Phys. **B944**, 114661 (2019), arXiv:1905.05464 [hep-ph].
[17] C. Simpson *et al.* (Super-Kamiokande), Astrophys. J. **885**, 133 (2019), arXiv:1908.07551 [astro-ph.HE].
[18] A. de Gouvea, Phys. Rev. **D63**, 093003 (2001), arXiv:hep-ph/0006157 [hep-ph].
[19] E. K. Akhmedov, P. Huber, M. Lindner, and T. Ohlsson, Nucl. Phys. **B608**, 394 (2001), arXiv:hep-ph/0105029 [hep-ph].